Influence of silicon addition and heat treatment on the microstructure and pitting behaviour of *AISI 304*

by C S M Lombardi and L V Ramanathan
Comissáo Nacional de Energia Nuclear, Instituto de Pesquisas Energeticas e Nucleares, Cidae Universitaria, Sáo Paulo, Brazil

THIS PAPER DISCUSSES the influence of silicon addition (0.9-4.7wt%) and heat treatment on the microstructure and pitting behaviour of *AISI 304* stainless steel in chloride solutions. The heat treatment consisted of annealing at 1200°C and 1300°C for one hour and subsequent ageing at 480°C, at 600°C, and at 700°C. The pitting-corrosion tests consisted of immersion in ferric chloride and anodic-polarization measurements in 3.5wt% sodium chloride. The delta-ferrite content of the alloys increased with silicon content and annealing temperature. Ageing resulted in transformation of the ferrite and formation of $M_{23}C_6$ precipitates. The overall pitting-corrosion rate decreased with silicon content. The pitting potential of the specimens increased with ferrite content and decreased with increasing ageing temperature and time.

The decrease in pitting corrosion with increase in silicon or ferrite content could be attributed to the formation of a more-protective surface film, containing both chromium and silicon. Increased pitting of the aged specimens was due to the formation of $M_{23}C_6$ precipitates, both within the ferrite grains and at the austenite/ferrite interface, and the consequent formation of chromium-depleted regions, which were susceptible to pit initiation.

Introduction

Austenitic stainless steels of the 300 series have been widely used due to their good mechanical properties, easy fabricability, and excellent general corrosion resistance. They are, however, susceptible to various forms of localized corrosion, especially pitting in chloride-ion containing environments. The pitting behaviour of austenitic stainless steels (SS) besides being dependent on environment-related factors such as pH, chloride-ion concentration, temperature, etc., is also dependent on alloy-related factors such as composition, microstructure, and the presence of precipitated phases and inclusions[1,2]. In terms of the effect of composition, the addition of alloying elements such as molybdenum, silicon, or vanadium to austenitic 18 chromium - 14 nickel SS reduced pitting susceptibility of the alloy[3,4]. Also, the addition of up to 4.45% silicon to 18 chromium - 8 nickel SS increased the resistance to pit initiation by a factor of 20, but decreased crevice-corrosion resistance[5].

The addition of silicon, a ferrite stabilizer, to an austenitic steel provokes the formation of delta (δ) ferrite[6]. The pitting potential (E_p), an electrochemical parameter indicative of pitting propensity of austenitic SS, was reported to shift to more-active values in the presence of small amounts of δ ferrite[7]. On the other hand, it has been reported[8] that the formation of up to 15% δ ferrite in heat-treated austenitic SS had an irregular effect on E_p[8]. The E_p of duplex steels with 50% δ ferrite shifted to values more noble than that of AISI 316 SS[7]. The pit-nucleation sites in δ-ferrite containing SS have been reported to be the δ phase, the austenite (γ) phase, or the δ/γ interface[8-10].

The reasons given to explain the different pit-initiation sites are varied. It has been suggested that the alloy-solidification process resulted in the depletion of chromium content in the interface region, making it more susceptible to pit initiation[3]. However, the difference in the chromium content between the two phases δ and γ was found[10] to be insufficiently low (approx. 1.5%), in agreement with the explanation[11] that preferential pitting of the δ/γ interface was due to segregation of impurities and/or the precipitation of new phases at these boundary regions.

It was further reported[12] that pits formed in the austenitic and the ferritic phases in duplex SS,

Alloy	Chemical composition (wt %)									
	C	Mn	P	S	Cr	Ni	Mo	N[p]	Ti	Si
A	0.070	1.39	0.019	0.008	19.30	9.00	0.09	532	0.002	0.92
B	0.067	1.52	0.017	0.007	19.10	9.60	0.09	550	0.003	1.51
C	0.069	1.53	0.019	0.009	18.90	9.40	0.09	512	0.002	2.46
D	0.068	1.55	0.020	0.008	18.60	9.10	0.10	521	0.002	4.73

p: ppm

Table 1. Chemical composition of the alloys used.

Heat treatment	Delta ferrite content (%) Alloy			
	A	B	C	D
1200° C 1h	3.2+0.5	4.5+0.1	10.6+1.0	45.0+2.5
480° C 10h	2.8	4.2+0.2	10.2+0.6	44.3+1.2
480° C 100h	2.3+0.2	2.3+0.07	9.0+0.8	33.0+0.7
600° C 1h	2.4+0.5	4.4+0.09	9.0+0.1	36.0+2.3
600° C 20h	2.2	3.8+0.3	9.3+0.6	35.0+3.0
700° C 1h	2.6	4.1+0.2	8.9+0.07	41.5+2.1
700° C 20h	2.2+0.07	3.7+0.3	8.3+0.4	31.0+0.5
1300° C 1h	8.2+0.4	15.3+1.1	32.0+3.3	67.7+3.7
480° C 10h	7.8	14.9+1.7	28.7+0.6	63..0+6.0
480° C 100h	7.2+1.4	11.7+1.0	20.7+4.0	59.0+6.1
600° C 1h	6.8+0.3	14.7+1.5	20.0+1.4	52.4+0.9
600° C 20h	6.2+0.6	10.6+1.6	19.3+1.5	48.3+5.0
700° C 1h	6.1+1.6	12.0+0.7	20.6+3.0	63.7+3.6
700° C 20h	6.2+0.6	7.1+0.4	18.0+1.0	39.2+1.1

Table 2. Delta-ferrite content of alloys annealed at 1200°C and 1300°C, and subsequently aged.

and preferential pitting in either phase was attributed to the partitioning of the alloying elements (chromium, molybdenum, and nitrogen) in the phases.

The pit-growth process, which is diffusion controlled, is quite different from the pit-initiation process[13]. The overall pitting behaviour is also influenced by heat treatments such as ageing, which provoke the precipitation of carbides[8]. This paper addresses the individual and combined influence of silicon addition to *AISI 304* and heat treatments, such as annealing and ageing of the alloys, on the pitting-corrosion behaviour.

Materials and methods

AISI 304 SS was melted in a vacuum induction furnace and Si added to obtain alloys A, B, C, and D with 0.9, 1.5, 2.5, and 4.7wt% silicon as shown in Table 1. The alloy specimens were subsequently heat treated in a vacuum; this consisted of (a) annealing at 1200°C and 1300°C for one hour followed by quenching in water, and (b) ageing the annealed specimens at (i) 480°C for 10 hours and 100 hours, (ii) 600°C for 1 hour and 20 hours, and (iii) 700°C for 1 hour and 20 hours followed by quenching. The ferrite content of the various alloys in the different heat-treated conditions was determined with a ferritoscope. Optical microscopic examination of the specimens was carried out on specimens prepared using standard metallographic practices. The specimens were electrolytically etched in 10% oxalic acid.

Two types of pitting tests were carried out: (a) immersion in ferric chloride solution for 96 hours, and (b) anodic-polarization measurements. The specimens for the immersion test were ground to

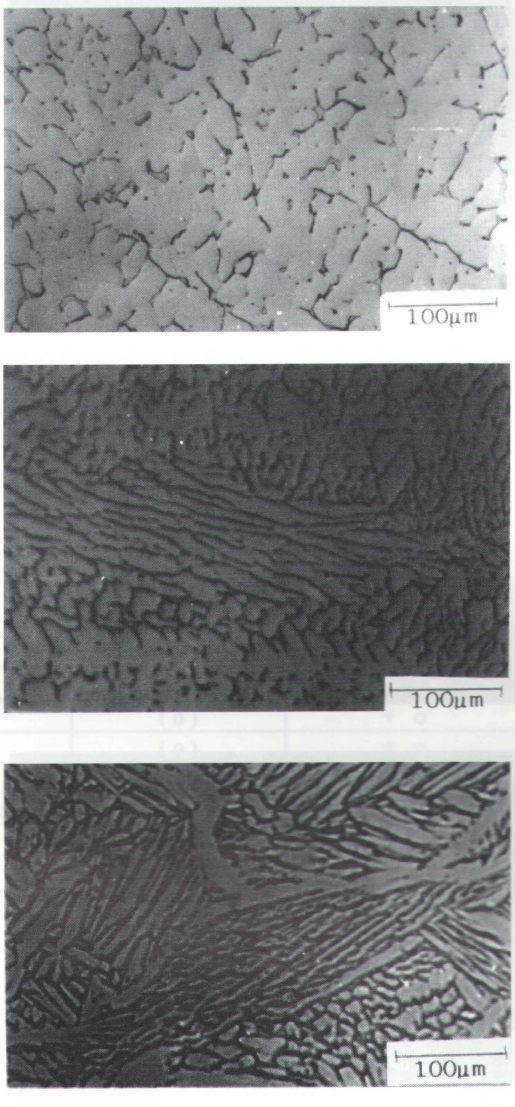

Fig.1(a-c: top-bottom). Optical micrographs of the as-cast alloys: (a) alloy A (b) alloy B (c) alloy C.

Fig.2 (a-e). Optical micrographs of:

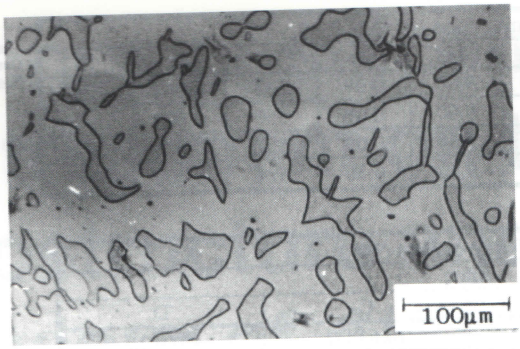

Fig.2a. Alloy C annealed at 1300°C for 1 hour.

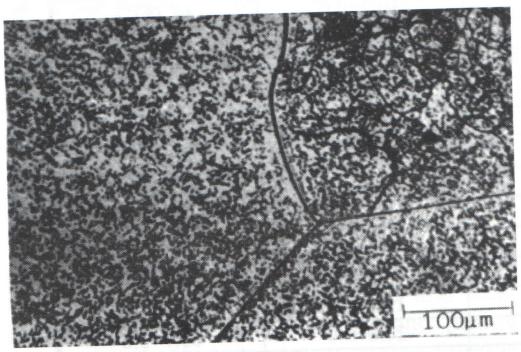

Fig.2b. Alloy D annealed at 1300°C for 1 hour.

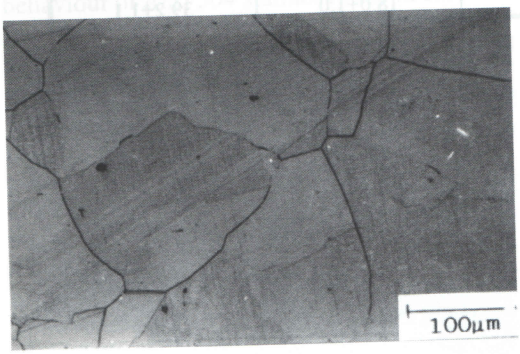

Fig.2c. Alloy A annealed at 1200°C and aged at 600°C for 1 hour.

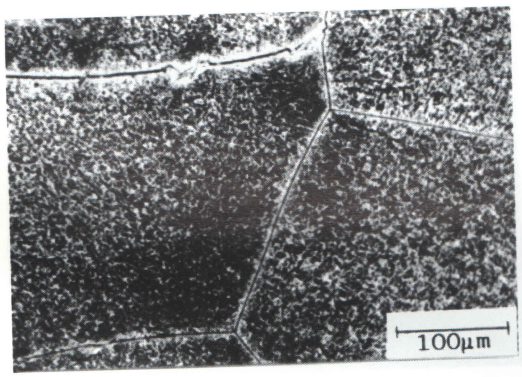

Fig.2d. Alloy D annealed at 1300°C and aged at 480°C for 10 hours.

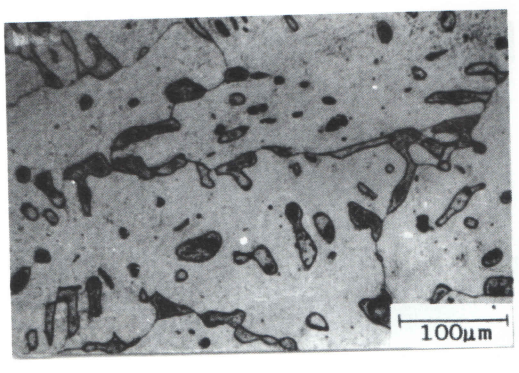

Fig.2e. Alloy B annealed at 1300°C and aged at 600°C for 20 hours.

600 grit; ultrasonically degreased, rinsed, and dried. A series of tests were conducted in which the ratio of specimen surface area to solution volume was varied. The pitting rates were determined from the weight loss.

The anodic potentiodynamic polarization measurements were carried out in aerated 3.5wt% sodium chloride solution at 25°C. The specimens were mounted in cold resin, ground to 600 grit, degreased, rinsed, and dried. They were then scanned from -100mV to +1000mV at a scan rate of 10mV/s in a standard corrosion cell, with a platinum counter electrode and a saturated calomel reference electrode. From the current-potential curves, the E_p was determined. The influence of chloride-ion concentration on pitting behaviour was also investigated by anodically polarizing the annealed specimens in sodium chloride solutions with 10ppm, 100ppm, and 1000ppm of chloride ions.

Measurements were also carried out to determine the pit-nucleation potential. This is the lowest potential below which pits do not nucleate after 16 hours' exposure to the chloride-ion containing solution. The specimens from the two types of corrosion tests were examined in an optical microscope as well as in a scanning-electron microscope coupled to an energy-dispersive analyzer.

Results and discussion

Delta-ferrite content and microstructure

The ferrite content of the different alloys is shown in Table 2. The ferrite content of the alloys increased with silicon content and with increase in annealing temperature. Upon ageing the annealed specimens, the ferrite content decreased; it also decreased with increase in ageing temperature or time at ageing temperature.

The microstructure of the as-cast alloys varied with Si content (as shown in Fig.1). Alloy A with 0.92% silicon revealed vermicular ferrite, and the high-silicon alloys showed increasing amounts of lathy ferrite. The various ferrite morphologies in the as-cast alloys could be attributed to differences in solid-state transformations[14,15]. Solidification of austenitic stainless steels can occur as primary austenite or as primary delta ferrite, depending on the position of the alloy composition relative to the liquidus line of the Fe-Cr-Ni ternary system. *AISI 304* solidifies as primary delta ferrite and subsequently undergoes massive transformation to austenite of near-normal composition[16].

In the absence of ferrite stabilizers, the amount of retained ferrite at room temperature is approximately 4-6%[16]. However, in the presence of a ferrite-stabilizing element such as silicon, a significant amount of ferrite is not transformed and is thus retained at room

Heat treatment	Alloy			
1200° C, 1h +	A	B	C	D
480°C 10h				
480°C 100h			(o)	(o)
600°C 1h	(*), #, o	(*), #, o	# o	# o
600°C 20h	(*), #, o	(*), #, o	# o	# o
700°C 1h	*, #, o	(*), #, o	# o	# o
700°C 20h	*, #, o	# o	# o	# o

Table 3. Microstructural changes upon ageing of the alloys annealed at 1200°C.
Note: (*) = precipitates at the austenite-austenite interface;
(#) = precipitates at the austenite-ferrite interface;
(o) = precipitates within the ferrite grain;
( ) = few precipitates.
Blank spaces signify an essentially similar structure to the as-annealed specimens.

temperature. The microstructure of the annealed specimens varied with alloy composition and the annealing temperature. In the alloys annealed at 1200°C, with increasing silicon, the ferrite phase increased from being tiny spots to islands, and then to large elongated islands. In alloy A annealed at 1300°C, the ferrite islands were bigger than those observed in the same alloy annealed at 1200°C, and alloy C with 2.5% silicon revealed coalesced ferrite grains as shown in Fig.2a.

The microstructure of alloy D with 4.7% silicon and annealed at 1300°C was, however, different and revealed large ferrite grains with a fine distribution of γ (shown in Fig.2b).

The effects of ageing on the annealed specimens are summarized in Table 3. The microstructure of the alloys annealed at 1200°C did not alter upon ageing at 480°C for 10 hours. Upon increasing the ageing time at 480°C, precipitates were observed in the high-Si alloys, mostly within the ferrite grains. The precipitates are probably $M_{23}C_6$, since their morphology is similar to that reported in the literature[8]. Ageing at 600°C resulted in formation of grain-boundary carbide precipitates also (as shown in Fig.2c). After longer times at 600°C and upon ageing at 700°C, carbide clusters were observed at the γ/δ and γ/γ boundaries and within the ferrite grains.

The influence of ageing on microstructure of the alloys annealed at 1300°C was different in some respects (as shown in Table 4). Upon ageing at 480°C for 10 hours, alloys C and D revealed $M_{23}C_6$ carbides at grain boundaries and within the ferrites. A precipitate-free zone close to the grain boundaries was also observed in alloy D (shown in Fig.2d). Increasing the time at 480°C resulted in overall decrease in the total amount of ferrite in alloys A-C. Ageing at 600°C for one hour resulted in formation of carbide precipitates, mostly within the ferrite grains in the different alloys. Upon increasing the ageing temperature to 700°C, or increasing time at both 600°C and 700°C, most of the carbides precipitated both at the γ/γ and γ/δ grain boundaries and within the ferrite grains (Fig.2e).

Pitting behaviour

Ferric chloride immersion test

All the alloys pitted in the ferric chloride solution. Fig.3 shows the pitting rate of the specimens as a function of silicon content. The pitting rate decreased with silicon content, and this decrease is more pronounced at high ratio of solution volume to specimen surface area. The

Heat treatment	Alloy			
1300°C 1h	A	B	C	D
480°C 10h			(o)	+ o
480°C 100h	(o)	(o)	(o)	+ o
600°C 1h	(o)	(o)	(o)	+ o
600°C 20h	* # o	* # o	# o	+ o
700°C 1h	(*) # o	# o	# o	+ o
700°C 20h	(*) # o	(*) # o	# o	+ o

Table 4. Microstructural changes upon ageing of alloys annealed at 1300°C.
Note: (*) = precipitates at the austenite-austenite interface;
(#) = precipitates at the austenite-ferrite interface;
(o) = precipitates within the ferrite grain;
( ) = few precipitates;
(+) = precipitates at the ferrite-ferrite interface.
Blank spaces signify an essentially similar structure to the as-annealed specimens.

Heat Treatment	Pitting potential (mV vs saturated calomel electrode)			
	Alloy			
	A	B	C	D
1200°C 1h	318	430	503	1253
480°C 10h	313	479	559	1307
480°C 100h	246	311	494	1227
600°C 1h	308	411	481	973
600°C 20h	166	223	238	917
700°C 1h	196	228	346	913
700°C 20h	118	220	332	>1500
1300°C 1h	494	643	>1500	>1500
480°C 10h	460	643	920	>1500
480°C 100h	389	566	1094	>1500
600°C 1h	265	552	653	921
600°C 20h	298	471	576	654
700°C 1h	310	471	617	1113
700°C 20h	208	497	508	853

Table 5. Pitting potentials in 3.5% sodium chloride at 25°C of specimens annealed at 1200°C, 1300°C and aged. Scan rate 10mV/sec.

extent to which the pitting rate decreased with silicon addition was significantly lower than that reported elsewhere[5]. The extent to which pitting rates in general decreased in small volumes of ferric chloride may be attributed to rapid saturation of the solution with complex metal chlorides and consequent stifling of the corrosion reaction.

Anodic-polarization tests

The E_p values of the alloys in 3.5%NaCl as a function of alloy composition and heat treatment are shown in Table 5. The E_p of the alloys increased with silicon content and upon annealing. The E_p values of the alloys annealed at 1300°C were higher than those annealed at 1200°C, indicating an increase in E_p with ferrite content of the alloys. The E_p of the aged specimens was less than that of the just-annealed specimens. The E_p also decreased with increasing ageing temperature and time. This decrease in E_p occurred as a result of carbide formation and consequent chromium depletion of the neighbouring regions. The values of pit-nucleation potential, E_{np}, of the alloys as a function of chloride-ion concentration are shown in Fig.4. The E_{np} of the alloys increased with silicon content and decreased with increasing chloride-ion concentration of the solution. Similar variations of E_p with chloride-ion concentration have been reported elsewhere[2].

A scanning-electron microscopic study of the specimen surfaces following exposure at E_p in sodium chloride for 30 seconds revealed a number of pits in the γ phase and in the δ phase. The δ/γ interfacial regions also showed a number of pits, and these grew into the γ phase (as shown in Fig.5). The increased susceptibility of the interfacial regions to pitting can be attributed to segregation effects[17]. The higher resistance of the ferrite phase to pitting is due to its higher chromium content[13]. The number and depth of the pits increased with increasing chloride-ion concentration.

General discussion

Heat-treatment effects

The equilibrium structure of an alloy such as *AISI 304* with approximately 0.5% silicon consists of γ at temperatures below 1200°C[18]. The equilibrium structure of the silicon-containing alloys studied here consisted of γ and ferrite. Above 1200°C in these alloys, more ferrite became stable and was retained upon quenching. The structure of the alloys aged at 480°C were not significantly different from those that were only annealed. Few carbide precipitates formed, due mostly to insufficient chromium mobility at this temperature. Upon ageing the silicon-containing alloys at 600/700°C, a significant part of the ferrite transformed to $M_{23}C_6$ and secondary γ, and the equilibrium structure of these alloys consisted of γ, δ, and $M_{23}C_6$.

The rate of decomposition of the ferrite phase increased due to chromium depletion, brought about by precipitation of $M_{23}C_6$ at the δ/γ grain boundaries. Although the carbon level in the alloy was relatively high, it is possible that the carbon available from the ferrite phase for carbide precipitation was quickly exhausted, and more carbon (necessary to continue to form the carbides) probably came almost exclusively from the γ phase. This eventually could have resulted in carbon depletion in the γ.

All the alloys in the different heat-treated conditions pitted in chloride-ion containing solutions. However, E_p, the pit-nucleation sites,

and the number of pits, varied with alloy composition and heat treatment. In the annealed silicon-containing alloys, with both the γ and the δ phases, the pits initiated preferentially in the γ phase and on the γ side near the γ/δ grain boundaries. Ageing of the alloys at 600°C resulted in an increase in the number of pits, and these pits formed in the γ, in the transformed δ regions, and near the carbides (possibly in the chromium-depleted regions). The chromium and carbon levels in the transformed ferrite regions (after carbide precipitation) were probably close to those of the γ phase, resulting thereby in both these regions being susceptible to pit initiation.

The pitting potentials of the alloys aged at 700°C were in some cases higher than those aged at 600°C. This could be attributed to differences in the chromium and carbon activities at these two temperatures. Similar results were reported earlier[8].

The role of silicon

The increase in pitting potential of the alloys with increase in silicon content and with increase in annealing temperature is directly related to the increase in δ-ferrite content. Since pits initiate at sites on the alloy surface where the surface film is weak or other heterogeneities are present, the increased resistance of the ferrite-containing alloys to pitting could be attributed to the formation of a more-protective surface film. The increase in E_p of alloys with increasing silicon can be attributed to the formation of a more pit-resistant surface film on the ferrite phase, which is rich in chromium and silicon[19]. Upon ageing, precipitation of $M_{23}C_6$ takes place. The decrease in E_p associated with ageing of the specimens is related to the formation of the precipitates and consequent depletion in chromium and carbon in the regions surrounding the precipitates. The film formed on these regions contains many more weak spots which are susceptible to pit initiation[10].

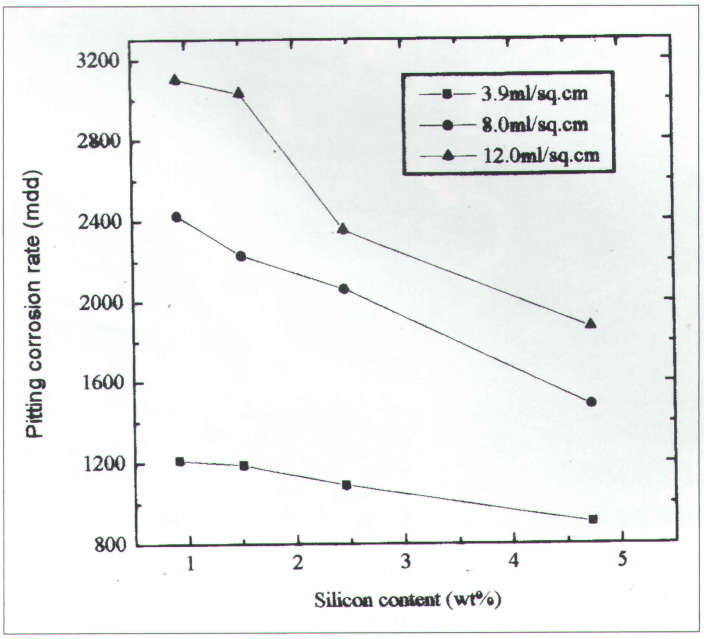

Fig.3. Pitting-corrosion rate of the different alloys in 10% ferric chloride solution as a function of silicon content in the alloys.

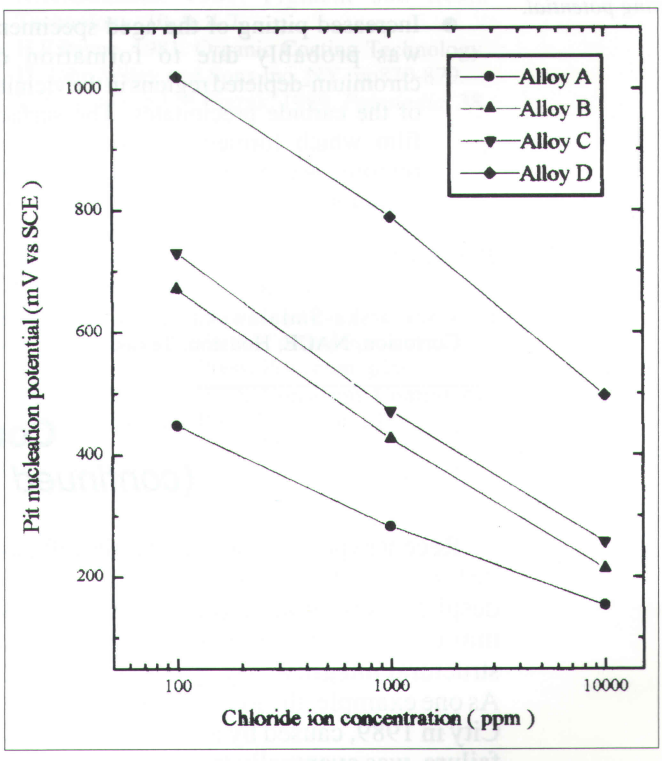

Fig.4. Pit-nucleation potential of the different alloys as a function of chloride-ion concentration in the electrolyte.

Conclusions

- The addition of silicon to *AISI 304* resulted in formation of the d-ferrite phase, which increased with increasing silicon content.
- Annealing the alloys at 1200-1300°C also resulted in an increase in the d-ferrite content. Ageing at and above 600°C resulted in precipitation of $M_{23}C_6$ at the austenite/ferrite boundaries and/or within the ferrite grains.
- The pitting-corrosion rates of the specimens decreased with increasing silicon content.
- The pitting potential of the alloys increased with ferrite content and decreased upon ageing.
- The pit-nucleation potential increased with silicon content of the alloy, and decreased with increasing chloride-ion concentration.

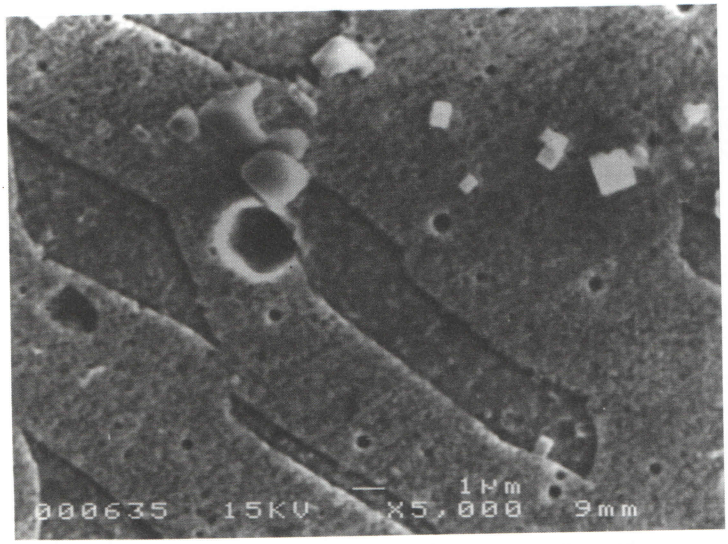

Fig.5. Scanning-electron micrograph of alloy C polarized for 30secs at its pitting potential.

- The increase in resistance to pitting with increase in silicon content could be attributed to the formation of a more-protective surface film, rich in silicon and chromium, on the ferrite grains.

- Increased pitting of the aged specimens was probably due to formation of chromium-depleted regions in the vicinity of the carbide precipitates. The surface film which formed on these depleted regions was more susceptible to pit initiation.

References

1. S.Szklarska-Smialawska, 1974. Localized Corrosion, NACE, Houston, Texas.
2. A.U.Malik, P.C.Mayankutti, N.A.Siddiqui, I.N.Andijani, and S.Ahmed, 1992. *Corrosion Sci.*, **33**, 1809.
3. N.D.Tomashov, G.P.Chemova and O.N.Markova, 1964. *Corrosion*, **20**, 166.
4. R.D.Davies and F.P.A.Robinson, 1989. *Corrosion*, **45**, 336.
5. B.E.Wilde, 1986. *Corrosion*, **42**, 147.
6. J.S.Armijo and B.E.Wilde, 1968. *Corrosion Sci.*, **8**, 649.
7. A.J.Sedriks, 1986. *Corrosion*, **42**, 376.
8. T.M.Devine, 1979. *J.Electrochem.Soc.*, **126**, 374.
9. T.P.S.Gill, U.Kamachi Mudali, V.Seetharaman, and J.B.Gnanamoorthy, 1988. *Corrosion*, **44**, 511.
10. P.E.Manning, C.E.Lyman and D.J.Duquette, 1980. *Corrosion*, **36**, 246.
11. M.A.Streicher, 1956. *J.Electrochem.Soc.*, **103**, 375.
12. R.Sriram and D.Tromanis, 1989. *Corrosion*, **45**, 804.
13. P.C.Pistorius and G.T.Burstein, 1992. *Corrosion Sci.*, **33**, 1885.
14. N.Suutala, T.Takalo, and T.Moisio, 1979. *Metallurgical Transactions*, A, **10A**, 512.
15. N.Suutala, T.Takalo and T.Moisio, 1979. *Metallurgical Transactions*, A, **10A**, 1183.
16. Y.Arata, F.Matsuda, and S.Katayama, 1976. *Transactions of Japanese Welding Res.Inst.*, **5**, 135.
17. J.B.Lumsden and P.J.Stoker, 1981. *Corrosion*, **37**, 60.
18. A.J.Sedriks, 1979. Corrosion of Stainless Steels, New York, John Wiley and Sons.
19. T.N.Rhodin, 1956. *Corrosion*, **12**, 123.

Comment

(continued from page 118)

Recent experience within the aircraft gas-turbine industry, however, has shown that, despite this rigorous approach, material and manufacturing flaws that can reduce structural integrity may remain undetected. As one example, the loss of a DC-10 at Sioux City in 1989, caused by an uncontained disk failure, was eventually traced to just such an undetected defect. The chance of flaws such as these being detected by standard laboratory mechanical testing procedures is miniscule. Consequently, operators of these engines face a dilemma with current design practices: either frequent and expensive inspection and possible replacement of parts, or the risk of catastrophe if a part is left too long in service.

As a result, the FAA requested the Aerospace Industries Association (AIA) to review available design procedures to see what supplemental methods could enhance safety, with the outcome that the Rotor Integrity Subcommittee of AIA recommended the programme now under way at SwRI.

"The probabilistic design code that the FAA has asked us to develop does not replace traditional 'safe-life' methods but provides an additional tool to minimize risk," says Dr Gerald R.Leverant, SwRI director of Power Generation Materials and manager of the FAA programme.

The first phase of the project is focussing on the presence of melt-related defects, known as 'hard alpha', found in titanium alloys. Hard alpha refers to small zones in the material microstructure which can be introduced at various stages in the melting history of the alloy. The zones often have

cracks or voids associated with them and can initiate the low-cycle fatigue cracks that contribute to disk failure.

Future phases of the project will apply the methodology to other types of titanium flaw, and to other widely-used rotor metals such as nickel alloys.

The protective propertiesof nickel ferrite

(*continued from page 139*)

the resulting highly anti-corrosive nature, as it is noted that there is a direct correlation between the electric resistance of a coating and the properties which protect against corrosion[19].

Conclusions

1. When a mixture of a-Fe_2O_3 and NiO in a molar ratio 1:1 is fired at 1155°C, a solid-state reaction occurs and nickel ferrite with a spinel structure is formed.

2. Evaluation of the specific properties of the prepared nickel ferrite powder showed that it can be satisfactorily used as a basic anti-corrosive pigment.

3. The results of Ni-ferrite/linseed-oil paints showed that there is a direct relationship between the concentration of the pigment and the properties protective against corrosion.

4. The anti-corrosion protective properties of Ni-ferrite-epoxy resin paints are excellent in all mixture ratios.

References

1. N.R.Barucha, 1965. *Nature*, **187**, 756.
2. M.M.Shirsalkar, V.N.Muley and M.A.Sivasamban, 1981. *Metal Finishing*, **79**, 7.
3. I.Sekine and T.Kota, 1987. *JOCCA*, **9**, 256-259.
4. I.Sekine and H.Suda, 1980. *Corrosion Engineering*, **37**, 423-430.
5. N.A.Eissa, A.A.Bahgat, A.H.Mohamed and S.A.Saleh, 1976. *J.Amer.Cer.Soc.*, **59**, 7, 327.
6. H.A.Bhuiya, J.Rahman and S.K.Paulit, 1980. *Bangladesh J.Sci.Ind.Res.*, **XV**, 1-4, 115-121.
7. A.A.Ibrahim and F.A.Healy, 1992. AMSE Transaction, **10**, 3, 1-14.
8. ASTM, Joint Committee on Powder Diffraction . Standers, file no. D 153-54.
9. E.Marsden, 1959. *JOCCA*, **42**, 119.
10. ASTM, D16A-83.
11. ASTM, D208-52T.
12. M.A.Abou-Khalil, S.M.El-Sawy and N.A.Ghanem, 1981. Pigment and Resin Technology, **10**, 9, 4-7.
13. H.F.Payne, 1981. Organic Coating Technology, **II**, John Wiley and Sons Inc, NY. pp870-879.
14. M.Svoboda and M.Prazak, 1989. *Paintindia*, **38**, 12, 57-60.
15. Modular Training Manual, **IIIa**, Selection and Industrial Training Adm.Ltd, London. p267.
16. J.Smit and H.J.P.Wijn, 1959. Ferrites. Philips Technical Library, N.V.Philips Gloeilampenfabriken, Eindhoven, Holland.
17. F.M.Speller, 1951. Corrosion. McGraw-Hill Book Co Inc, NY. 3rd edn., ch2, p38.
18. H.Jr.Leidheiser, 1979. Corrosion Control by Coatings. Science Press, Princeton. p29.
19. H.Jr.Leidheiser, 1979. Corrosion Control by Coatings. Science Press Princeton. p143.